Preprints of the 19th World Congress
The International Federation of Automatic Control
Cape Town, South Africa. August 24-29, 2014

Car attitude control by series mechatronic suspension ⋆

Carlos Arana * **Simos A. Evangelou** * **Daniele Dini** **

* *Depts. of Mechanical and Electrical and Electronic Engineering, Imperial College London, London, SW7 2AZ, UK (e-mail: carlos.arana-remirez10@imperial.ac.uk, s.evangelou@imperial.ac.uk).*
** *Dept. of Mechanical Engineering, Imperial College London, London, SW7 2AZ, UK (e-mail: d.dini@imperial.ac.uk)*

Abstract: This paper investigates the potential of the Series Active Variable Geometry Suspension (SAVGS) to control chassis roll and pitch motions during cornering and combined cornering and braking events. A cascaded control scheme that drives the four actuators (one per wheel) independently and respects all physical and design limitations is presented. The control system is thereafter applied to a specific SAVGS configuration and tested through nonlinear simulation of a full vehicle model of a generic high performance sports car. A wide set of simulation results corresponding to standard open loop maneuvers is shown, providing insight on the performance of the SAVGS, its requirements, operation, and influence on the directional response of the vehicle. These results suggest that the SAVGS is well suited to controlling chassis attitude motions in this class of vehicles.

Keywords: Active vehicle suspension, vehicle dynamics, attitude control, cascade control, servomechanisms.

1. INTRODUCTION

Electronics, electrics and mechatronics accounted for 20-25% of the total price of an average car five years ago (Isermann, 2008), and this figure has probably risen sharply. Among chassis subsystems, Electro-Mechanical Brakes (EMB), mechatronic steering systems and mechatronic active suspensions are receiving significant attention (Schöner, 2004). The development of these technologies forms a positive feedback loop, as there are many synergies that can be exploited. They all benefit from the availability of higher bus voltages, sensors and other components can be shared, they can work together towards improving the directional response of the vehicle, and ultimately, they contribute towards the long term goal of a fully electric vehicle, where no hydraulic systems are needed.

This paper studies the potential of a specific fully active, series mechatronic suspension, in terms of roll and pitch attitude control of the chassis. The main contributions are *a*) the presentation of a simple but effective control strategy for blending pitch and roll control that satisfies all physical and design actuator constraints and *b*) the presentation of a full set of detailed simulation results obtained with a high fidelity full vehicle model for standard open loop test maneuvers.

The remainder of this paper is organized as follows: Section 2 briefly describes the single-link variant of the Series Active Variable Geometry Suspension (SAVGS); Section 3 deals with the application of this technology to chassis attitude control; Simulation results for a generic high performance sports car are included and discussed in detail in Section 4; Final remarks and an outline of future work are provided in Section 5.

2. CHARACTERISTICS OF THE SINGLE-LINK VARIANT OF THE SAVGS

The single-link variant of the SAVGS, which has been presented in (Arana et al., 2012, 2013), is shown in Fig. 1. A single mechanical link is introduced between the upper end of the passive spring-damper unit and the chassis. Point G is the joint of the single-link with the chassis, and point F is the joint of the single-link with the strut end. The spring-damper force as well as the installation ratio (Dixon, 2009) are altered due to the rotation of the single-link. The actuation torque, T_{SAVGS}, is applied to the single-link about a longitudinal axis that goes through point G. Considering the equilibrium position as the zero angle reference (left hand side configuration in Fig. 1), the single-links installed on the right (left) wheels operate within 0 and $\rho_{max} \leq 180°$ ($-\rho_{max} \geq -180°$) with respect to the x-axis of the vehicle (SAE J670e convention: longitudinal, pointing forward).

The actuator is fixed to the chassis and comprises a Permanent Magnet Synchronous Motor (PMSM) connected to an epicyclic gearbox [1] . It can be installed either along the longitudinal axis of the car if an in-line gearhead is used, or along any direction in the transverse plane of the vehicle if a right angle gearbox is selected. More details regarding

⋆ This work was supported by the UK Engineering and Physical Sciences Research Council and by Imperial Innovations.

[1] The same actuator type is being considered for its application in other active chassis systems, such as EMBs (Ki et al., 2013) and steer-by-wire (Wang et al., 2013).

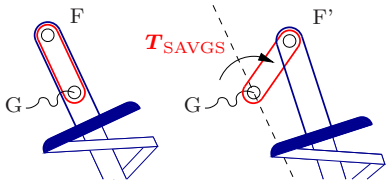

Fig. 1. Single-link variant of the SAVGS.

key design aspects, component selection and dimensioning can be found in (Arana et al., 2013).

Some important advantages of this active mechatronic suspension that works in series with the passive spring and damper include: *a*) it is fail safe, *b*) it does not increase the unsprung mass, *c*) it uses conventional electro-mechanical components, *d*) it has energy regeneration capabilities, and *e*) several packaging alternatives are possible.

3. METHODOLOGY FOR CHASSIS ATTITUDE CONTROL

Keeping the attitude of the chassis within allowable limits is important in order to *a*) avoid degrading the quality of the ride, *b*) avoid increasing the load transfer during acceleration/braking and turning maneuvers, *c*) avoid excessive changes in the camber angle of the wheels, and *d*) maintain the desired level of aerodynamic forces on the vehicle. Each of these aspects may lead to different pitch and roll chassis motion requirements. For example, a negative pitch angle (diving) in a race car may be beneficial while braking due to increased aerodynamic drag forces, but it may be undesirable in a passenger car in terms of comfort and safety.

A control scheme for tracking pitch and roll references is presented in this section. Although fixed target values have been assumed, this control could easily be combined with an additional outer loop that determined the optimum roll and pitch angles depending on the driving conditions (e.g. in terms of human perception, (Buma et al., 2008)).

The share of roll resisting moment between axles has an effect on the directional stability and responsiveness of the vehicle. This is determined by the relative stiffnesses of the front and rear suspensions elements (passive and/or active), as well as by the heights of the roll centers (see Fig. 2). The presented control focuses solely on chassis attitude tracking and displays a fixed roll compensation share between axles; further developments of the control strategy, such as those presented in (Gerhard et al., 2005), could be incorporated if a certain directional behavior was to be provided by the active suspension.

The outer control loop for one of the four actuators is shown in Fig. 3. The pitch angle reference, θ^*, and roll angle reference, ϕ^*, are tracked by PD controllers in blocks *A1* and *A2*. These generate increments, $\Delta\rho^*_\theta$ and $\Delta\rho^*_\phi$, that are added to the base reference, ρ^*_b, in order to produce a single-link angle reference, ρ^*_u. This value is subsequently saturated to ensure that the single-link remains within the desired range of angular positions, and tracked by the internal position and current control loops of the actuator (see Fig. 4). The output of the actuator is the torque applied to the single-link, T_{lss}.

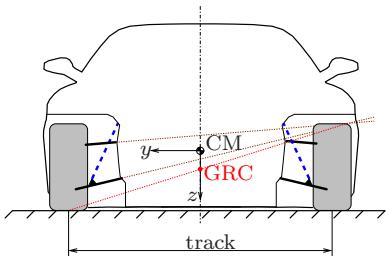

Fig. 2. Front suspension geometry in the *y*-*z* plane. The height difference between the geometric roll center of each axle and the center of mass of the chassis gives an indication of the roll moment that needs to be compensated by the compliant suspension elements in that axle (i.e. spring and damper) during cornering.

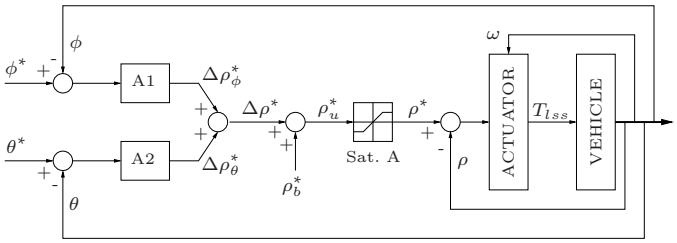

Fig. 3. Outer loops in the attitude control scheme.

Numbering the four corners of the vehicle as: 1 - front left, 2 - front right, 3 - rear left, and 4 - rear right, the equations in blocks *A1* and *A2* are given in (1) and (2) respectively, where K refers to control gains, subscripts P and D to proportional and derivative, and superscripts f and r to front and rear.

$$\Delta\rho^*_\phi = \begin{cases} -K^f_{P_\phi}(\phi^* - \phi) - K^f_{D_\phi}\dfrac{d(\phi^* - \phi)}{dt} & \text{for act. 1 \& 2} \\ -K^r_{P_\phi}(\phi^* - \phi) - K^r_{D_\phi}\dfrac{d(\phi^* - \phi)}{dt} & \text{for act. 3 \& 4} \end{cases} \tag{1}$$

$$\Delta\rho^*_\theta = \begin{cases} -K^f_{P_\theta}(\theta^* - \theta) - K^f_{D_\theta}\dfrac{d(\theta^* - \theta)}{dt} & \text{for act. 1} \\ K^f_{P_\theta}(\theta^* - \theta) + K^f_{D_\theta}\dfrac{d(\theta^* - \theta)}{dt} & \text{for act. 2} \\ K^r_{P_\theta}(\theta^* - \theta) + K^r_{D_\theta}\dfrac{d(\theta^* - \theta)}{dt} & \text{for act. 3} \\ -K^r_{P_\theta}(\theta^* - \theta) - K^r_{D_\theta}\dfrac{d(\theta^* - \theta)}{dt} & \text{for act. 4} \end{cases} \tag{2}$$

The base reference, ρ^*_b, has two main functions: to ensure that *a*) the single-links remain at or close to the desired offset angles at low levels of longitudinal and lateral acceleration, and *b*) that steady-state pitch and roll angle errors are zero. In order to maintain the single-links close to their offset position, ρ^*_b must be set to ρ_{off} in at least one of the vehicle axles. On the other hand, ρ^*_b should match the actual single-link angles in at least one of the axles if the steady state errors are to be kept at zero. Thus, ρ^*_b values must depend on the level of horizontal acceleration, $|a_{hor}|$, and need to be different for each axle. The expressions that have been used in this study are given in (3), where a_{th1} and a_{th2} are tunable constants.

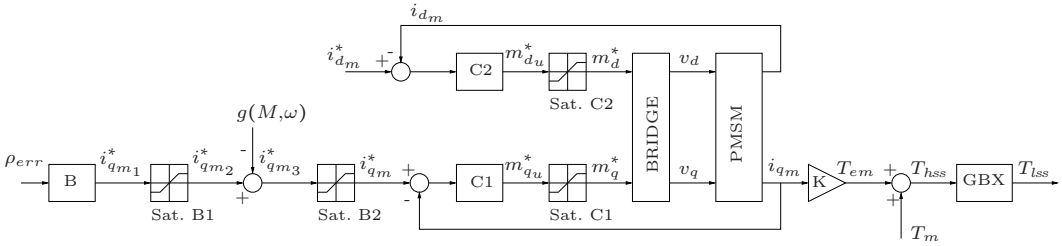

Fig. 4. Position control of the actuator, where ρ_{err} is the error in single-link position; $i^*_{q_{m1}}$, $i^*_{q_{m2}}$ and $i^*_{q_{m3}}$ are references for the magnetizing component of the q-current (computed by taking into account current, torque and speed limitations); $i^*_{d_m} = 0$ is the reference for the magnetizing component of the d-current; and $m^*_{d_u}$, $m^*_{q_u}$, m^*_d and m^*_q are the unsaturated and saturated modulation indexes that determine the voltage that is subsequently applied by the bridge converter to the d and q phases of the PMSM (v_d and v_q). The magnetizing component of the q-current, i_{q_m}, is responsible for the generation of the electromagnetic torque, T_{em}, which combined with the torque due to mechanical losses in the motor, T_m, leads to the torque applied to the high speed shaft of the gearbox, T_{hss}. Finally, the gearbox model, which includes a fixed gear ratio and efficiency coefficient, produces the desired output, which is the torque generated in the output or low speed shaft of the gearbox, T_{lss}, and applied to the single-link.

$$\rho_b^* = \begin{cases} -\rho_{off} + \rho_{cf} \cdot (\rho_1 + \rho_{off}) & \text{for act. 1} \\ \rho_{off} + \rho_{cf} \cdot (\rho_2 + \rho_{off}) & \text{for act. 2} \\ \rho_3 & \text{for act. 3} \\ \rho_4 & \text{for act. 4} \end{cases} \tag{3a}$$

$$\rho_{cf} = \frac{2}{\pi} \arctan\left[a_{th1} \cdot \left(\frac{|a_{hor}|}{a_{th2}} \right)^2 \right] \tag{3b}$$

Full details of the actuator modeling and control can be found in (Arana et al., 2013). Particular attention has been paid to ensuring that all physical and design limitations of the actuators are respected, and that their dependency on the operating conditions is taken into account. These limitations include voltage, current and power limitations of the motor, torque limitations of the gearbox, and speed limitations of the motor and the gearbox. The control strategy for one of the actuators is outlined in Fig. 4.

4. SIMULATION RESULTS FOR A HIGH PERFORMANCE SPORTS CAR

The designed controller is incorporated into a nonlinear, full vehicle multibody model of a high performance sports car and tested through simulation of standard open loop maneuvers. Previous work (Arana et al., 2012, 2013) described the vehicle model and focused on pitch mitigation during acceleration and braking maneuvers of various severities. The current contribution tackles both roll and pitch control during cornering events. Cases studied include steady-state cornering as defined in (ISO 4138:2004), lateral transient response as defined in (ISO 7401:2011), and braking in a turn as defined in (ISO 7975:2006). The results included in this section correspond to pitch and roll angle references equal to zero, i.e. the control objective is to keep the chassis parallel to the road surface. However, as it has been previously pointed out, this may not be the optimum control target at all times and for all vehicle classes. Therefore, the aim of the results presented here is simply to assess the achievable roll and pitch motion correction with a reasonably sized SAVGS system.

4.1 Vehicle and actuator parameters

Simulations are carried out with one specific vehicle, representative of the high performance sports car class.

Table 1. Main vehicle parameters

Parameter	Units	Value
Total mass/Sprung mass	kg	1525/1325
Wheelbase/Height of center of mass	mm	2600/424
Track (front/rear)	mm	1669/1615
Weight distribution (front/rear)	%	43/57
Spring stiffness (front/rear)	N/mm	92/158
Roll center height (front/rear)	mm	275/300
Tire stiffness (front & rear)	N/mm	275
Installation ratio (front & rear)	-	0.56

Table 2. SAVGS parameters

Parameter	Units	Value
Single-link length (front/rear)	mm	15/11
PMSM (front & rear)	-	Kollmorgen AKM33H
Gearbox (front & rear)	-	Danaher UT075-40
Mass (front & rear)	kg	~6/actuator
Power limit (front & rear)	W	500/actuator
DC bus voltage (front & rear)	V	160

Key parameters used in the simulation are given in Table 1. The SAVGS setup corresponds to that presented in (Arana et al., 2013), with a power limit of 500 W per actuator imposed by the control system. Main parameter values are shown in Table 2.

4.2 Steady-state cornering

This initial set of simulation results provides valuable information regarding the maximum roll compensation that can be achieved in quasi static cornering circumstances, as well as on the effect of the control strategy on pitch and on the directional behavior of the vehicle.

Simulation runs are performed according to test method number 1, as specified in (ISO 4138:2004). This open loop maneuver consists of driving the vehicle in a circle of prescribed radius (R=100 m), at increasing speeds. The virtual driver needs to adjust the steering wheel angle in order to ensure that the car accurately follows the desired path. This is achieved by converting the target path radius, R, into a yaw rate reference, r^*, as a function of the forward speed of the vehicle, v_{fwd}, as in (4). Then the required steering wheel speed, $\dot{\delta}_{sw}$, can be calculated as a function of the yaw rate error as in (5). Of course, the

Table 3. Control parameters for the outer loop

Parameter	Units	SAVGS #1	SAVGS #2	SAVGS #3
ρ_{off}	rad	0	1.2	1.2
$K^f_{P_\phi}$	-	500	500	5000
$K^r_{P_\phi}$	-	5000	5000	500

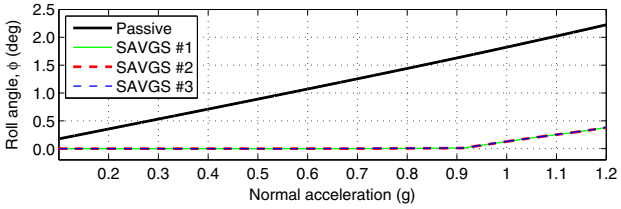

Fig. 5. Roll angle as a function of the normal acceleration throughout a quasi steady-state cornering maneuver.

steering wheel needs to remain within its operational range at all times, i.e. $-\delta_{sw}^{max} \leq \delta_{sw} \leq \delta_{sw}^{max}$.

$$r^* = \frac{|v_{fwd}|}{R} \tag{4}$$

$$\dot{\delta}_{sw} = K_r \left(r^* - r\right) \cdot \min\left(1, \delta_{sw}^{aux}\right) \tag{5a}$$

$$\delta_{sw}^{aux} = 2 - \frac{|\delta_{sw}| - \delta_{sw}^{max}}{||\delta_{sw}| - \delta_{sw}^{max}|} - \frac{\left(r^* - r\right)\delta_{sw}}{|\left(r^* - r\right)\delta_{sw}|} \tag{5b}$$

Results are presented for the vehicle equipped with the passive suspension, and for the same system retrofitted with the SAVGS and three different sets of control parameters: without offset, with offset and more roll compensation at the rear, with offset and more roll compensation at the front (see Table 3). In all active cases roll is much more weighted than pitch, and $K^f_{P_\theta} = 12$, $K^r_{P_\theta} = 2.4$, $K^f_{D_\theta} = 4.8$, $K^r_{D_\theta} = 0.96$, and $K^f_{D_\phi} = K^r_{D_\phi} = 0$.

Fig. 5 shows the roll angle evolution with respect to normal accelerations (i.e. horizontal acceleration perpendicular to the trajectory of the center of mass) of up to 1.2 g. The original passive vehicle displays a linear relationship, with a slope of ~1.8 deg/g. The SAVGS manages to keep total roll angle at zero for normal accelerations up to 0.9 g. Roll angle increases at a rate of ~1.3 deg/g for larger values of normal acceleration.

Pitch evolution with respect to normal acceleration is shown in Fig. 6. The increasing side slip angle of the vehicle induces a gradual increment of the pitching angle. In the passive case, pitch is small and remains an order of magnitude smaller than the roll angle. In the active case, the single-links prioritize keeping the roll angle well under control, even if that implies some degradation of the pitch response. Controller #2 performs best, maintaining pitch angle at zero up to 0.7 g of normal acceleration. In all cases, pitch angle becomes significant for normal accelerations greater than 1 g. This highlights the trade-off that is necessary at high normal, longitudinal, or normal and longitudinal accelerations, when the actuators are starting to lose control authority (single-links are approaching either the maximum or minimum allowable angular position). In this paper, roll control has been given priority over pitch control. The desired balance between these two objectives can be achieved by adjusting the relative gains in the control blocks *A1* and *A2*.

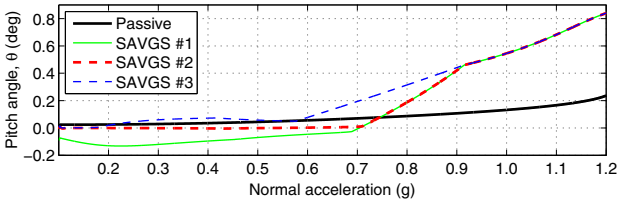

Fig. 6. Pitch angle as a function of the normal acceleration throughout a quasi steady-state cornering maneuver.

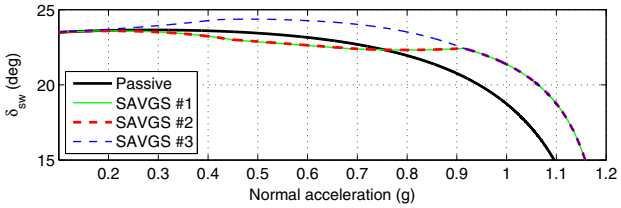

Fig. 7. Steering wheel angle vs. normal acceleration throughout a quasi steady-state cornering maneuver.

Moreover, the relative gains for roll control between the front and rear actuators determine the share of load transfer that is compensated by each axle. Higher gains at the front (rear) axle will increase understeer (oversteer) behavior, increasing (reducing) directional stability but reducing (increasing) responsiveness to driver's inputs. This becomes apparent in Fig. 7, where the steering wheel angle required to keep the car in a 100 m radius circle is shown. The SAVGS affects the directional response at normal accelerations up to 0.9 g. At higher normal accelerations, all single-links have reached the boundary of their allowable angular positions and the response is similar to that of the passive vehicle (clearly oversteering).

4.3 Transient lateral response

Two maneuvers according to (ISO 7401:2011) have been used to test the performance of the SAVGS during transient lateral motion.

Step steer: the first event is a left hand step steer. The vehicle is driven in a straight line with a constant throttle position that corresponds to 100 km/h. The steering wheel is then rotated at a rate of 500 deg/s up to an angle that, in steady cornering conditions at 100 km/h, would lead to a normal acceleration equal to a_n^{ss}. Results are shown for a_n^{ss}=8 m/s^2, with steering wheel change starting at t=1 s.

Pitch and roll evolutions are shown in Fig. 8 and Fig. 9. Roll is perfectly kept under control with the three controllers, although, as expected, transient response is better in the case of operating the single-links from an offset position. Pitch evolution is slightly worse than in the passive case, but it is still good, as it is maintained below 0.2 deg at all times.

Fig. 10 shows the time evolution of the normal acceleration. The vehicle equipped with the SAVGS and controllers #1 and #2 displays a similar response to that of the passive car. In the case of a front bias in the roll control, the peak normal acceleration reached is ~5% smaller. This highlights how the SAVGS control may work together

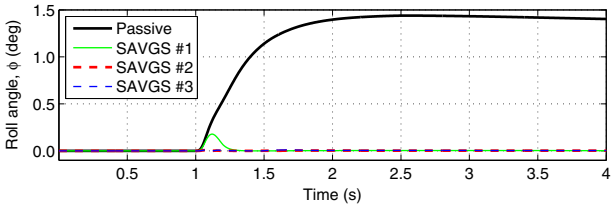

Fig. 8. Roll angle evolution for a step steer maneuver leading to a_n^{ss}=8 m/s^2, as defined in (ISO 7401:2011).

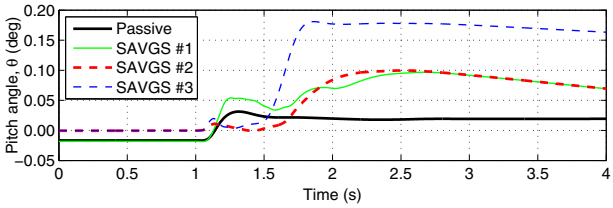

Fig. 9. Pitch angle evolution for a step steer maneuver leading to a_n^{ss}=8 m/s^2, as defined in (ISO 7401:2011).

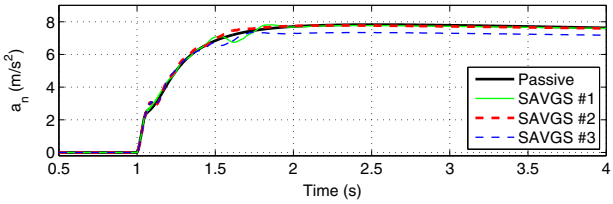

Fig. 10. Normal acceleration for a step steer maneuver leading to a_n^{ss}=8 m/s^2, as defined in (ISO 7401:2011).

with other active chassis systems in order to adjust the directional response and stability of the vehicle.

The operating points of all actuators in the case of controller #2 are shown in Fig. 11, along with actuator envelopes for peak and continuous operation (thick lines), and constant output mechanical power lines. The control scheme successfully maintains the operating points within the allowable range for continuous operation. The rear right actuator is the one that reaches the power limit when in driving mode (the gap to the 500 W mechanical power line is due to the losses in the actuator, as the power limit is imposed in terms of electrical power consumption), as it aims to compensate both pitch and roll. Inner actuators remain mainly in the regenerative region.

Continuous sinusoidal steer input: The second transient lateral maneuver tested is a continuous sinusoidal steer input with fixed throttle position. The initial test speed is 100 km/h and the amplitude of the steering wheel cycles is such that a normal acceleration of a_n^{ss} would be obtained if maintained in a steady cornering event at 100 km/h. Four different levels of steering wheel amplitude have been studied (a_n^{ss}=2, 4, 6 and 7 m/s^2), and input frequencies have been swept at 0.2 Hz intervals in the 0.2 Hz to 2.6 Hz range. Results are shown for controller #2 only.

Fig. 12 shows that the amplitude of the normal acceleration in the passive and active cases is very similar at all frequencies. As expected, normal acceleration amplitudes decrease with steering wheel input frequency. Moreover, normal acceleration amplitudes are lower than the corresponding a_n^{ss} values even at low frequencies because the forward speed drops once the steering begins.

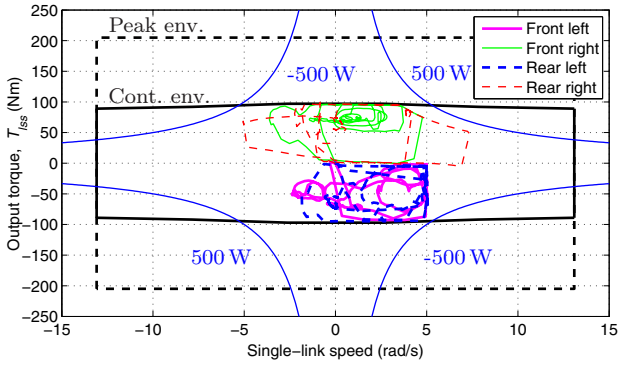

Fig. 11. Output torques provided by the actuators vs. single-link speeds for a step steer maneuver leading to a_n^{ss}=8 m/s^2, as defined in (ISO 7401:2011).

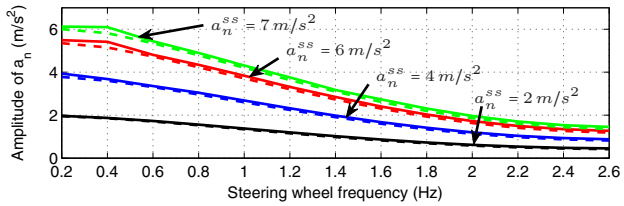

Fig. 12. Normal acceleration amplitudes for continuous steering wheel sinusoid inputs of various amplitudes and frequencies. Passive vehicle response shown with dashed lines, and SAVGS #2 shown with solid lines. The amplitude is obtained as half the difference between the maximum and minimum normal acceleration values during a 10-cycle period, starting in the fourth cycle to ensure that responses have stabilized.

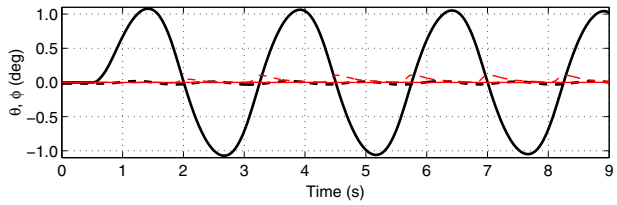

Fig. 13. Roll (solid) and pitch (dashed) angle evolution for the passive (black, thick) and SAVGS #2 (red, thin) configurations during a continuous steering wheel sinusoid input at 0.4 Hz and a_n^{ss}=7 m/s^2.

Roll is effectively kept at zero throughout the simulations, and peak pitch angle is maintained below 0.2 deg in all cases. A sample result for roll and pitch evolution in one of the most demanding cases is shown in Fig. 13.

Another important aspect that needs consideration in this set of maneuvers is power consumption. The controller imposes a soft constraint of 500 W on the electric power flow from/to each actuator. Yet average power consumption is significantly smaller due to energy regeneration. In the worst case, average power consumption per actuator remains below 300 W/4=75 W. This is shown in Fig. 14.

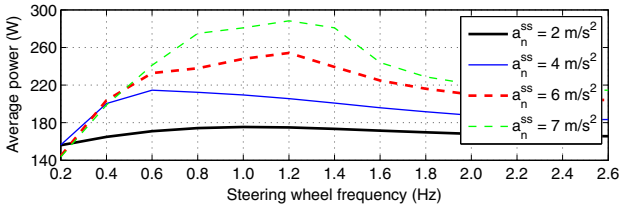

Fig. 14. Average total power consumption for continuous steering wheel sinusoid inputs of various amplitudes and frequencies. The average power is calculated within a 10-cycle period, starting in the fourth cycle to ensure that responses have stabilized.

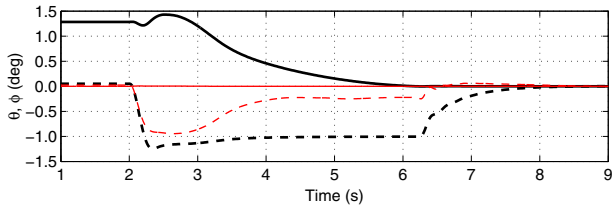

Fig. 15. Roll (solid) and pitch (dashed) angles for the passive (black, thick) and SAVGS #2 (red, thin) configurations during a brake in turn event.

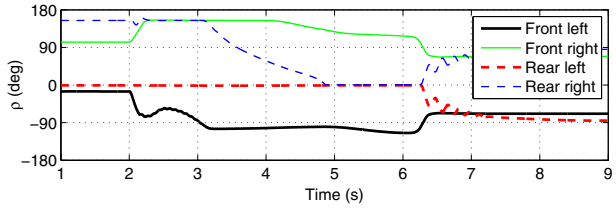

Fig. 16. Single-link angles for a brake in turn event.

4.4 Braking from steady-state circular motion

The final set of results correspond to the brake in turn maneuver described in (ISO 7975:2006). The car is initially driven in a left hand turn of radius R=100 m with a normal acceleration of 7 m/s^2, and then, keeping the steering wheel position constant, it is decelerated at a rate of 6 m/s^2 until it reaches a forward velocity of 1 m/s..

Pitch and roll angle evolution for the passive and active (controller #2) cases are depicted in Fig. 15. The roll angle is kept at zero, whilst the pitch angle is also significantly reduced with respect to the passive case.

Single-link angles are shown for this left hand turning event in Fig. 16. Before the deceleration phase begins, the rear right single-link is already at its maximum allowable angle, whereas the rear left is at its minimum allowable angle (in absolute value). When braking begins, the front actuators start compensating for pitch, and as speed and therefore normal acceleration is reduced, the rear right actuator becomes free to contribute towards pitch reduction.

5. CONCLUSION AND FUTURE WORK

A pitch and roll attitude control strategy for the SAVGS that takes into account actuator dynamics as well as current, voltage, power, speed and torque limitations has been presented. Standard open loop maneuvers have been used to test this control strategy within a nonlinear, full vehicle model representative of the high performance sports car class. Detailed simulation results have been included. With reasonably sized actuators, the SAVGS and corresponding control system is able to keep roll motion at zero for normal acceleration levels of up to 0.9 g, and to remain well behaved at higher acceleration levels. It is also able to successfully tackle combined pitch and roll events, such as the brake in turn maneuver.

The proposed control system offers a simple way of limiting the maximum electric power flows from/to each actuator. Moreover, the regenerative capabilities of this mechatronic suspension lead to very low average power consumption, as it has been shown at various frequencies in the continuous steering wheel sinusoid input test.

Future work on the SAVGS regarding chassis attitude control will include the development of alternative control strategies as well as its dimensioning and application to different vehicle classes.

REFERENCES

Arana, C., Evangelou, S.A., and Dini, D. (2012). Pitch angle reduction for cars under acceleration and braking by active variable geometry suspension. In *51st IEEE Conference on Decision and Control (CDC)*, 4390–4395.

Arana, C., Evangelou, S.A., and Dini, D. (2013). Series active variable geometry suspension for road vehicles. *IEEE/ASME Trans. Mechatronics*. In review.

Buma, S., Kajino, H., Takahashi, T., and Doi, S. (2008). Consideration of a human dynamic characteristic and performance evaluation of an electric active suspension. In *IEEE/ASME International Conference on Advanced Intelligent Mechatronics (AIM)*, 1030–1036.

Dixon, J. (2009). *Suspension geometry and computation*. Wiley Online Library.

Gerhard, J., Laiou, M.C., Mönnigmann, M., Marquardt, W., Lakehal-Ayat, M., Aneke, E., and Busch, R. (2005). Robust yaw control design with active differential and active roll control systems. In *Proceedings of the 16th IFAC World Congress on Automatic Control, Prague, Czech Republic, July*, 4–8.

Isermann, R. (2008). Mechatronic systems – innovative products with embedded control. *Control Engineering Practice*, 16(1), 14 – 29.

ISO 4138:2004 (2004). Passenger cars - Steady-state circular driving behaviour - Open-loop test methods.

ISO 7401:2011 (2011). Road vehicles - Lateral transient response test methods - Open-loop test methods.

ISO 7975:2006 (2006). Passenger cars - Braking in a turn - Open-loop test method.

Ki, Y., Lee, K., Cheon, J., and Ahn, H. (2013). Design and implementation of a new clamping force estimator in electro-mechanical brake systems. *International Journal of Automotive Technology*, 14(5), 739–745.

Schöner, H.P. (2004). Automotive mechatronics. *Control Engineering Practice*, 12(11), 1343 – 1351.

Wang, H., Man, Z., Shen, W., and Zheng, J. (2013). Robust sliding mode control for steer-by-wire systems with ac motors in road vehicles. In *8th IEEE Conference on Industrial Electronics and Applications (ICIEA)*, 674–679.